Title
PARTICLE PRODUCTION BY RELATIVISTIC HEAVY IONS

Author
Steiner, Herbert.

Publication Date
1974-09-01

Presented at the International Conference on
High Energy Collisions Involving Nuclei,
Trieste, Italy, September 9-13, 1974.

LBL-3613

PARTICLE PRODUCTION BY RELATIVISTIC HEAVY IONS

Herbert Steiner

September 1974

Prepared for the U. S. Atomic Energy Commission
under Contract W-7405-ENG-48

DISCLAIMER

LBL-3613

PARTICLE PRODUCTION BY RELATIVISTIC HEAVY IONS*

Herbert Steiner

Department of Physics and
Lawrence Berkeley Laboratory
University of California
Berkeley, California 94720

Invited talk at International Conference on High Energy Collisions Involving Nuclei, Trieste, Italy, September 9 - 13, 1974

---

* Prepared for the U.S. Atomic Energy Commission under Contract W-7405-ENG-48

PARTICLE PRODUCTION BY RELATIVISTIC HEAVY IONS*

H. M. Steiner,
Lawrence Berkeley Laboratory,
University of California
Berkeley, California, USA.

In this talk I would like to review briefly some recent experiments involving energetic "heavy" ions at Berkeley. These experiments were all carried out at the Bevatron-Bevalac Facility at the Lawrence Berkeley Laboratory. The term "heavy" ions here means particles with baryon number $B \geq 1$. The emphasis will be primarily on projectile and target fragmentation studies at energies of 1 & 2 GeV per nucleon.

At the outset it is useful to recall some elementary but practically important kinematical facts associated with the type of experiments to be discussed here. The use of energetic nuclear projectiles makes possible the study of (projectile) fragmentation processes in which the fragments have very low energy relative to the fragmenting object. Such fragments will be <u>fast</u> in the laboratory and <u>highly collimated in the forward direction</u>. At the energies considered here the projectile and target fragments are usually kinematically quite distinct. For example at 2 GeV/nucleon the rapidity gap, Y, between target and projectile is about 2 units whereas the typical width of the single particle rapidity distributions, δy, associated with the fragmentation of target (or projectile) nucleus is only $\delta y \cong 0.3$. By comparison, at the ISR for collisions between beams of 25 GeV protons $Y \cong 8$ and the single particle inclusive pion spectra associated with one of the protons have $\delta y \simeq 2$. It is thus tempting to try to apply theoretical concepts such as scaling, factorization and limiting fragmentation also to high energy nuclear processes. Not only are concepts important in characterizing high energy interactions, but also in helping us to get a clearer picture of the structure of the colliding objects. In the case of nuclei, high energy collisions afford a new and powerful tool for studying nuclear structure (e.g. constituent momentum distributions) and nuclear correlations.

The physics interest in high energy nuclear collisions goes beyond trying to determine high energy interaction mechanisms or how constituents move within a nucleus. The basic interaction cross sections are important ingredients in calculations of cosmic ray source abundances and lifetimes. The possibility of producing high energy hypernuclei (and even superstrange nuclei) has already stimulated some preliminary experimental activity.[1] Perhaps the most exciting possibilities lie in potential discovery of completely new and heretofore unknown phenomena resulting from head-on collisions between heavy nuclei. Recent theoretical speculations about superdense, superheavy nuclei by Lee and Wick,[2] and about the formation of abnormally high nuclear densities by Greiner et al.[3] and by Chaplaine et al.[4] will undoubtedly stimulate a flurry of experimental activity. I will leave it to Professor Lee to tell you more about some of these very interesting ideas.

II. The Bevalac - A Brief Status Report

The Bevalac is a mating of the SuperHILAC (HILAC ≡ Heavy Ion Linear ACcelerator) and the Bevatron. The SuperHILAC, which can accelerate almost all types of ions to energies of about 8 MeV/nucleon, is used to inject heavy ions into the Bevatron. It is connected to the Bevatron by a 230 m long transfer line. In the Bevatron the ions can be accelerated to any predetermined energy below 2.5 GeV/nucleon and then extracted in an external beam. A schematic sketch of the general layout is shown in figure 1. The expected particle fluxes are shown in figure 2. As can be seen from this figure the fluxes of particles heavier than iron are expected to be vanishingly small. This limitation is a consequence of the relatively poor vacuum in the Bevatron ($p \simeq 2 \times 10^{-7}$ Torr). A beam of fully stripped ^{12}C ions was successfully accelerated through the whole system at the beginning of August 1974. In the 3rd week of August a beam of $\sim 10^8$ ^{20}Ne ions was extracted at 2.1 GeV/nucleon. Since that time (Sept. 1974) ^{40}Ar has also been accelerated to 2.1 GeV/nucleon and extracted into the external beam channel (2×10^6 particles per pulse).

Plans for the future involve accelerating heavier ions, increasing the reliability of operation, and making it possible to "time-share" the SuperHILAC beam between the Bevalac and the low energy heavy ion users of the SuperHILAC. If money can be found attempts will be made to improve the vacuum system to make possible very heavy ion (Pb, U) acceleration in the Bevatron.

III. Some (Selected) Experimental Results

A. Projectile Fragmentation Studies: Single Particle Inclusive Spectra at 0° (B. B. Cork, H. H. Heckman, D. E. Greiner, P. J. Lindstrom and F. S. Bieser) (LBL).

Although many different types of nuclear projectiles were fragmented on a variety of targets in the course of these experiments, the case of ^{16}O projectiles at 2.1 GeV/nucleon on a ^{12}C target will serve to illustrate the general nature of the results. The objectives of this experiment were to measure the momentum distributions of the various fragments and to determine how the fragmentation cross section depended on fragment type. Fragment identification and momentum determination was accomplished by magnetic deflection, dE/dx and time-of-flight. A more complete description of the methods used can be found in reference 5, which describes an earlier experiment of the same type. The results of this earlier experiment indicated that the momentum distributions of all of the observed fragments relative to the rest frame of the ^{16}O projectile could be fit with a gaussian of the form $\exp[-p^2/2m_\pi^2]$, as shown in figure 3. This result was unexpected and defied a simple explanation. The more accurate and extensive recent experiment reported here again shows that except for protons the momentum distributions of the fragments are generally well fit by a gaussian. For example the ^7Be spectrum is shown in figure 4. However Cork et al. now find that the width of the gaussian distribution depends on the fragment type. The dependence of the width of the gaussian distributions on the (Z,A) of the fragment is shown in figure 5. The solid curve corresponds to a width $\sigma \propto \sqrt{A_{frag}(A_{proj} - A_{frag})/A_{proj}}$ which is the functional form expected from almost all simple theoretical models, e.g. statistical models by Feshbach and Huang[(6)] and by A. S. Goldhaber,[(7)] a thermodynamic model by A. S. Goldhaber,[(7)] and a model based on a quantum mechanical sudden approximation by Lepore and Riddell.[(8)]

B. Target Fragmentation Studies: Single Particle Inclusive Spectra of Low Energy Fragments at Various Angles (A. M. Zebelman, A. M. Poskanzer, J. D. Bowman, R. G. Sextro and V. E. Viola) (LBL).

The primary objective of this experiment was to compare the fragmentation of ^{238}U induced by relativistic protons, deuterons, and alpha particles. The following reactions were studied:

(a) $p + {}^{238}U \rightarrow X + \ldots$ (4.8 GeV), (b) $d + {}^{238}U \rightarrow X + \ldots$ (2.1 GeV/n) and (c) $\alpha + {}^{238}U \rightarrow X + \ldots$ (2.1 GeV/n), where X represents a fragment produced in the interaction. The measured fragments were stopped in solid state detectors. Identification was made by measuring both dE/dx and E. In figure 6(a) we see that the ratio for producing various fragments by deuterons and protons is independent of fragment type or fragment energy. The ratio of alpha to proton induced fragmentation of ${}^{238}U$ is shown in figure 6(b). In this case there is a marked dependence on both fragment type and momentum. It is unlikely that the difference in total bombarding energy is responsible for this effect, since it is known that the fragmentation cross sections induced by protons are almost independent of proton energy for $T_p > 2$ GeV. In figure 7 we see that the tails of the fragmentation spectra induced by alphas (solid lines) are consistently higher than the proton-induced spectra (dashed lines) when both spectra are normalized to the same value at the peak. Interpretation in terms of an evaporation model would require a nuclear temperature approximately 2-3 MeV higher for alphas than for protons, i.e. an alpha particle tends to deposit more energy in ${}^{238}U$ than does a proton.

C. Target Fragmentation Studies: Single Particle Inclusive Spectra at All Angles up to Energies of ∿1000 MeV (H. J. Crawford, P. B. Price, J. Stevenson and L. W. Wilson) (UC Berkeley).

In this experiment Au was bombarded with 25 GeV ${}^{12}C$ ions. The energy and angular distributions of fragments with $5 \leq Z \leq 9$ were studied with Lexan (Plastic) detector stacks. The energy range of detected fragments extended beyond those of Zebelman et al. One of the main objects of this experiment was to look for possible hydrodynamic effects in high energy nuclear collisions. The velocities of the detected fragments ranged from ∿0.1 c to ∿0.4 c which probably includes the range of velocities of acoustic or plasma waves in nuclear matter. Figure 8 shows differential cross sections as a function of energy at various angles to the beam for fragments of Be, B, C, N, O, F, Ne, Na, and Mg. The energy distribution of carbon fragments emitted at various angles from a gold target is shown in figure 9. The secondary peak near 55 MeV/nucleon is particularly intriguing. It is clear that such a peak is difficult to reconcile with a simple evaporation mechanism. Are we seeing here the effects of a nuclear shock wave? At this point it is premature to attribute these preliminary results to any specific mechanism, but it will be interesting to study such spectra under a wide variety of kinematic conditions in order to establish the importance of "hydrodynamic" effects in this collision of high energy nuclei. Furthermore the very simple and novel experimental technique of using plastic detectors to identify energetic nuclear fragments is applicable also in the search for possible superheavy nuclei.

D. Projectile Fragmentation and Pion Production by Light Relativistic Ions on Nuclei (J. Papp, J. Jaros, L. Schroeder, H. Steiner, J. Staples, A. Wagner, and J. Wiss) (LBL).

In this experiment the main emphasis was on π^- production by energetic protons, deuterons, alpha particles and ^{12}C ions on various nuclear targets (Be, C, Cu, Pb). Positive pions as well as baryonic fragments were also studied. The primary objective was to determine to what extent very energetic pions, i.e. pions with energies considerably larger than those which result from simple nucleus collisions would be produced by alpha and deuteron projectiles. Do the observed pion spectra result from nucleon-nucleon collisions or are more complicated processes also important?

A magnetic spectrometer was used to momentum analyze the fragments, and this together with measurements of time-of-flight, dE/dx, and Čerenkov light provided particle identification. The results of π^- production by protons of various energies on a Be target are shown in figure 10. When these results are replotted as in Fig.11(a) (invariant cross section $E/k^2(d^2\sigma/d\Omega dk)$ vs the scaling variable $x' = k^*_{\parallel}/(k^*_{\parallel})_{max}$ all of the π^- spectra tend to fall on top of each other. Similar measurements made at higher energies (12, 19 and 24 GeV/c protons on Be) also fall on the same curve. Scaling behavior, where the pion yield does not depend on energy but only on a scaling variable x' (at fixed $k_\perp$) is familiar in very high energy elementary particle processes. The remarkable feature of the present data is that scaling persists at least approximately down to 1 GeV. It is worth pointing out that in contrast to the scaling of the π^- data, the π^+ do not scale very well at the lower energies.

Negative pion production cross sections for 2.1 GeV/nucleon protons, deuterons, and alphas incident on carbon are shown in figure 12. Two features are obvious: (1) The heavier the projectile the larger the cross section. In fact, for 1 GeV π^- the ratio of cross sections $\sigma_\alpha:\sigma_d:\sigma_p$ is about 10:5:1. (2) The heavier the projectile the higher the maximum energy of the observed pions. When the invariant cross sections for producing negative pions by deuterons and alpha particles of 1.05 and 2.10 GeV per nucleon on a carbon target are replotted in terms of x' (figure 11) we again see that scaling seems to be quite well satisfied. However, the distributions fall more steeply with x' as the mass of the projectile increases. These results indicate that a relatively loosely bound composite system of nucleons such as a deuteron or alpha particle tends not to transfer a large fraction of its total kinetic energy to individual pions. The results on π^- production by deuterons differ from those of Baldin et al.[9] who find that the ratio

$$R(x') \equiv \frac{\sigma(d + Cu \to \pi^- + \text{anything})}{\sigma(p + Cu \to \pi^- + \text{anything})}$$

is independent of x' in the interval $0.5 \leq x' \leq 0.9$. It is unlikely that the different kinematic conditions of the two experiments can account for this discrepancy.

The dependence of the pion production cross section on the mass of the target can be parameterized in the form $\sigma \propto A^n$. A plot of n as a function of pion momentum for 2.1 GeV/nucleon deuteron and alpha projectiles is shown in figure 13. The $A^{1/3}$ dependence for $k_\pi > 1$ GeV/c suggests peripheral production. In all cases the ratio of π^-/π^+ production by both deuterons and alphas on carbon is consistent with unity, indicating that charge symmetry is not violated.

The importance of effects in which several nucleons in an energetic nuclear projectile act cooperatively to produce pions has been estimated by comparing the experimental results to calculations based on a model in which all pions are produced in individual <u>nucleon-nucleus</u> collisions. In this model it is assumed that in a reaction of the type $a + A \to \pi + \text{anything}$

$$\sigma^\pi_{aA}(\vec{p}_a,\vec{k}_\pi) = \sum_{n=1}^{a} \int W_{an}(\vec{p}_a,\vec{p}_n)\sigma^\pi_{nA}(\vec{p}_n,\vec{k})d^3\vec{p}_n$$

where $W_{an}(\vec{p}_a,\vec{p}_n)$ is the momentum distribution of the nucleons inside of the projectile transformed to the lab system. I will leave it to Professor Bertocchi to discuss this model in more detail. Let me just quote some results. The predictions of the model in the case of deuteron projectiles are shown together with the data points in figure 14(a). The fits reproduce quite well the general behavior of the measured cross sections for fast pions as a function of pion momentum. There are no free parameters. These results disagree with the conclusions of Baldin et al.[9] who claim to be unable to fit their data with such a model.

The case of alphas is complicated by the fact that the single nucleon momentum distribution is not well known. From electromagnetic form factor experiments one can deduce a charge distribution, but it is difficult to translate this to the momentum distribution $|\phi_\alpha(q)|^2$. As a first approximation $\phi_\alpha(q)$ was obtained from the Fourier transform of the square root of the nuclear charge distribution.[10] $W_{\alpha n}(\vec{p}_\alpha,\vec{p}_n)$ was then obtained by transforming $|\phi_\alpha(q)|^2$ to the lab system. The results are shown in figure 14(b). Although the general trends of the data are reproduced by the model, quantitatively the agreement is not good. At this point it is impossible to know whether this is due to a poor choice for $W_{\alpha n}(\vec{p}_\alpha,\vec{p}_n)$ or to a breakdown of the model. Further work is in progress for both deuterons and alphas.

Time does not permit a full discussion of all of the fragmentation spectra measured in this experiment. A few examples are shown in figures 15 and 16. In figure 15 we see that the single particle inclusive proton, deuteron, and ^{3}He spectra resulting from the interaction of 2.1 GeV/n alphas on carbon show very clear peaks associated with projectile fragmentation plus "central plateaus" at lower values of the rapidity y. As expected the heavier the projectile the more narrow the width of the "projectile fragmentation peak." Figure 16 shows a direct comparison between the single particle proton spectra as a function of rapidity for 2.1 GeV/nucleon deuterons and alphas fragmenting on carbon. The width of the proton distribution from the deuterons is narrower than that from the alphas, reflecting the fact that the momentum distributions of protons in deuterons is not as broad as that in alpha particles. The point in showing these examples is to indicate the potential usefulness of high energy fragmentation processes in studying constituent abundances, momentum distributions and correlations.

E. Measurement of Total Nucleus-Nucleus Cross Sections with Energetic Light Nuclei (J. Jaros, L. Anderson, O. Chamberlain, R. Fuzesy, J. Gallup, W. Gorn, L. Schroeder, S. Shannon, G. Shapiro, H. Steiner, A. Wagner, J. Wiss) (LBL).

Recently a systematic study was undertaken to measure σ_T for all combinations of p, d, ^4He and ^{12}C on each other at about 1 and 2 GeV/nucleon. The object was to test various theoretical predictions and in particular to see how well the factorization relation $\sigma_{AA}\sigma_{BB} = \sigma_{AB}{}^2$ is satisfied in such interactions. It is worth noting that this relationship between cross sections is expected to hold to a good approximation even in a non-factorizable geometric model as long as the masses of A and B are not very different. The main experimental and theoretical problem associated with this experiment is how to separate the nuclear and coulomb effects. This problem becomes especially acute in the case of ^{12}C on ^{12}C. The data are now being analyzed.

F. Preliminary Study of ^{12}C Fragmentation on a Lucite Target in the LBL Streamer Chamber (G. K. Chang, W. Gorn, Y. T. Oh, J. Ozawa, R. Po, B. Shen: U.C. Riverside) (L. Schroeder, H. Steiner: LBL)

A short test run was recently made to investigate the potential usefulness of the LBL streamer chamber as a detector for high energy fragmentation processes. The streamer chamber has some obvious advantages for certain types of interactions (4π solid angle, good multi-particle efficiency, it can be triggered, ionization information may be obtainable, it has reasonable momentum resolution since it operates in a field of 14 kilogauss). Various trigger schemes were tried in this test, and some examples of the type of picture obtained are shown in figures 17 and 18. It seems clear that this technique is well suited to this type of physics and is likely to play an important role especially in studies of multiparticle final states (e.g. multi-pions).

IV. Conclusions

I have tried to give a brief resumé of some of the experiments that have been carried out at the Bevatron during the last year or so. It is a program which already has yielded some interesting results and which is likely to provide new insight into nuclear structure and high energy interaction mechanisms. With the advent of the Bevalac some of the exciting speculations about possible new phenomena resulting from head-on collisions between really heavy nuclei should start to be susceptible to experimental investigation in the near future.

REFERENCES

* Work done under the auspices of the U.S. Atomic Energy Commission.

1. T. Bowen, G. Cable, D. A. Delise, E. W. Jenkins, R. M. Kalbach, K. J. Nield, R. C. Noggle and A. E. Pifer; private communication (a short description of this experiment can be found in ref. 5, p. 405).
2. T. D. Lee, Abnormal Nuclear States and Vacuum Excitations, unpublished.
3. Werner Scheid, Hans Müller, and Walter Greiner, Nuclear Shock Waves in Heavy-Ion Collisions, Phy. Rev. Lett. 32, 741 (1974).
4. G. F. Chaplaine, N. H. Johnson, E. Teller, M. S. Weiss, Highly Excited Nuclear Matter, Phys. Rev. D8, 4302 (1973).
5. H. Heckman,"High-Energy Heavy Ions: A New Area for Physics Research," High-Energy Physics and Nuclear Structure, Proceedings of the Fifth International Conference on High-Energy Physics and Nuclear Structure, Uppsala, Sweden, June, 1973, edited by Gunnar Tibell; North-Holland Publishing Company, 1974.
6. H. Feshbach and K. Huang, Phys. Lett. 47B, 300 (1973).
7. A. S. Goldhaber, Statistical Models of Fragmentation Processes, presented at High Energy Heavy Ion Summer Study, Berkeley, California, July, 1974; unpublished.
8. J. Lepore and R. Riddell, Fragmentation of Heavy Nuclei at High Energies, LBL Report 3086 (unpublished).
9. A. M. Baldin, S. B. Gerasimov, H. Guiordenescu, V. N. Zubarev, L. K. Ivanova, A. D. Kirillov, V. A. Kuznetsov, N. S. Moroz, B. B. Radomanov, V. N. Ramzhin, V. S. Stavinskii, and M. I. Yatsuta, Sov. J. Nucl. Phys. 18, 41 (1974).
10. R. F. Frosch, J. S. McCarthy, R. E. Rand and M. R. Yearian, Phys. Rev. 160, 874 (1967).

FIGURE CAPTIONS

1. Schematic view of Bevalac showing SuperHILAC injector, transfer line, and Bevatron.
2. Expected particle fluxes in Bevalac External Beam as a function of atomic number.
3. Momentum distributions of various fragments relative to the rest frame of the ^{16}O projectile as determined in the original measurements of Heckman et al.[5] The solid curve is a gaussian with a width of $\sigma = m_\pi$.
4. Momentum distribution of ^7Be fragments relative to the rest frame of the ^{16}O projectile obtained in the more recent experiment of Cork, et al. (see section III-A). The solid curve is a gaussian function with a width σ = 165 MeV. Data of Cork, et al. (III-A).
5. The widths of the gaussian functions used to fit the observed fragment momentum distributions as a function of fragment type. The solid curve was obtained from the calculations of Lepore and Riddell.[8] Experiment of Cork, et al. (see section III-A).
6. (a) The ratio $\frac{\sigma(d + {}^{238}U \rightarrow (Z,A) + \text{anything})}{\sigma(p + {}^{238}U \rightarrow (Z,A) + \text{anything})}$ at 90° as a function of fragment energy for various types of fragments (Z,A) obtained by Zebelman et al. (see section III-B).

   (b & c) The ratio $\frac{\sigma(\alpha + {}^{238}U \rightarrow (Z,A) + \text{anything})}{\sigma(p + {}^{238}U \rightarrow (Z,A) + \text{anything})}$ at 90° as a function of fragment energy for various fragment types (Z,A). Experiment of Zebelman et al. (see section III-B).
7. Comparison between the fragmentation yields as a function of fragment energy induced by 2.1 GeV/nucleon alpha particles and 4.8 GeV protons interacting with a ^{238}U target. The various spectra have been arbitrarily normalized to be the same at their respective peaks. Experiment of Zebelman et al. (see section III-B).
8. Cross sections as a function of fragment energy for producing various types of fragments at 25° in the reaction $^{12}C + Au \rightarrow (Z,A)$ + anything for 2.1 GeV/nucleon carbon projectiles. Experiment of Crawford, et al. (see section III-C).
9. Energy distribution of ^{12}C fragments produced at various angles in the reaction $^{12}C + {}^{198}Au \rightarrow {}^{12}C$ + anything for 2.1 GeV/nucleon ^{12}C projectiles. Experiment of Crawford et al. (see section III-C).
10. Differential cross section, $d^2\sigma/d\Omega dk_\pi$, as a function of pion momentum, k_π, for the reaction $p + {}^{12}C \rightarrow \pi^-$ + anything at $\theta_{lab}=2.5°$. The curves are only intended to guide the eye along spectra obtained at various proton energies. Data of Papp, et al. (see section III-D).
11. (a) Invariant cross section $E/k^2\ d^2\sigma/dkd\Omega$ as a function of the scaling variable $x' = k^*_\pi/(k^*_\pi)_{max}$ for the reaction $p + Be \rightarrow \pi^-$ + anything at various proton energies. Data of Papp, et al. (see section III-D).

    (b) Same as (a) except deuteron and alpha projectiles instead of protons.
12. Cross section $d^2\sigma/dk_\pi d\Omega$ as a function of pion momentum, k_π, for producing π^- at θ_{lab} = 2.5° in the reactions $\begin{Bmatrix} p \\ d \\ \alpha \end{Bmatrix} = Be \rightarrow \pi^-$ + anything at 2.1 GeV/nucleon. Data of Papp et al. (see section III-D).
13. Dependence of the pion production cross section on the mass of the target as a function of pion momentum. Plotted is n (assuming $\sigma \propto A^n$) versus k_π. Data of Papp, et al. (see section III-D).

14. Comparison of the measured π^- production cross sections $d^2\sigma/d\Omega dk_\pi$ as a function of pion momentum with the model described in the text. Data of Papp et al. (see section III-D).
(a) $d + {}^{12}C \rightarrow \pi^- +$ anything for 1.05 and 2.10 GeV/nucleon deuterons
(b) $\alpha + {}^{12}C \rightarrow \pi^- +$ anything for 1.05 and 2.10 GeV/nucleon alphas.
15. Invariant cross section, $E/k^2\, d^2\sigma/dkd\Omega$ as a function of fragment rapidity for proton, deuteron, ^3H and ^3He fragments produced by 1.05 GeV/nucleon alpha particle projectiles on Be. Data of Papp et al. (see section III-D).
16. Comparison of the single particle inclusive proton rapidity distributions resulting from the fragmentation of 2.1 GeV/nucleon deuteron and alphas on a beryllium target. Data of Papp et al. (see section III-D).
17. Example of streamer chamber picture showing the interaction of a .87 GeV/n carbon ion in a lucite target. UCR-LBL Streamer Chamber Collaboration (see section III-F).
18. Another example of a streamer chamber picture showing the fragmentation of a .87 GeV/n carbon ion into three alpha particles as a result of an interaction in a lucite target. UCR-LBL Streamer Chamber Collaboration (see section III-F).

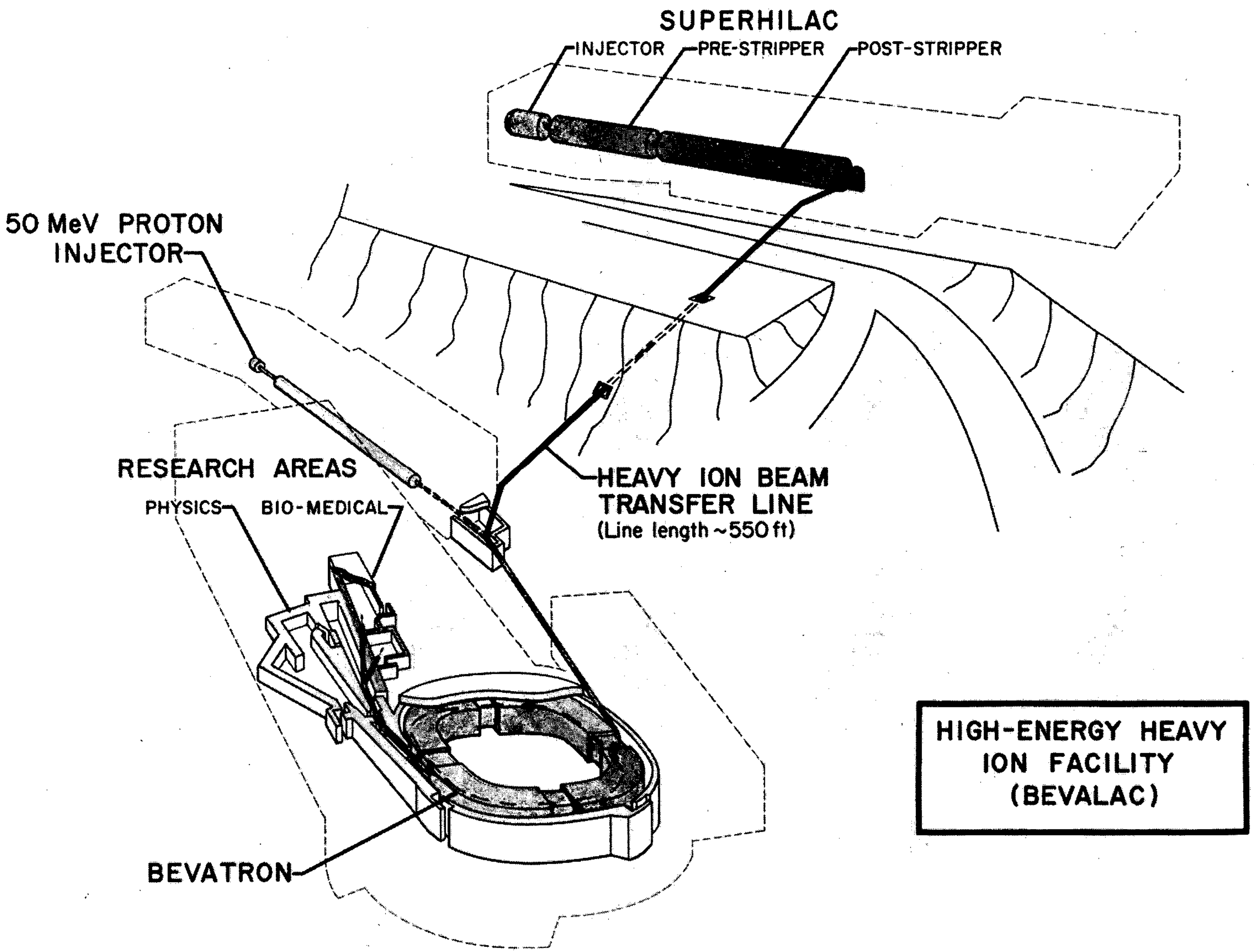

CBB 729-4520

Fig. 1

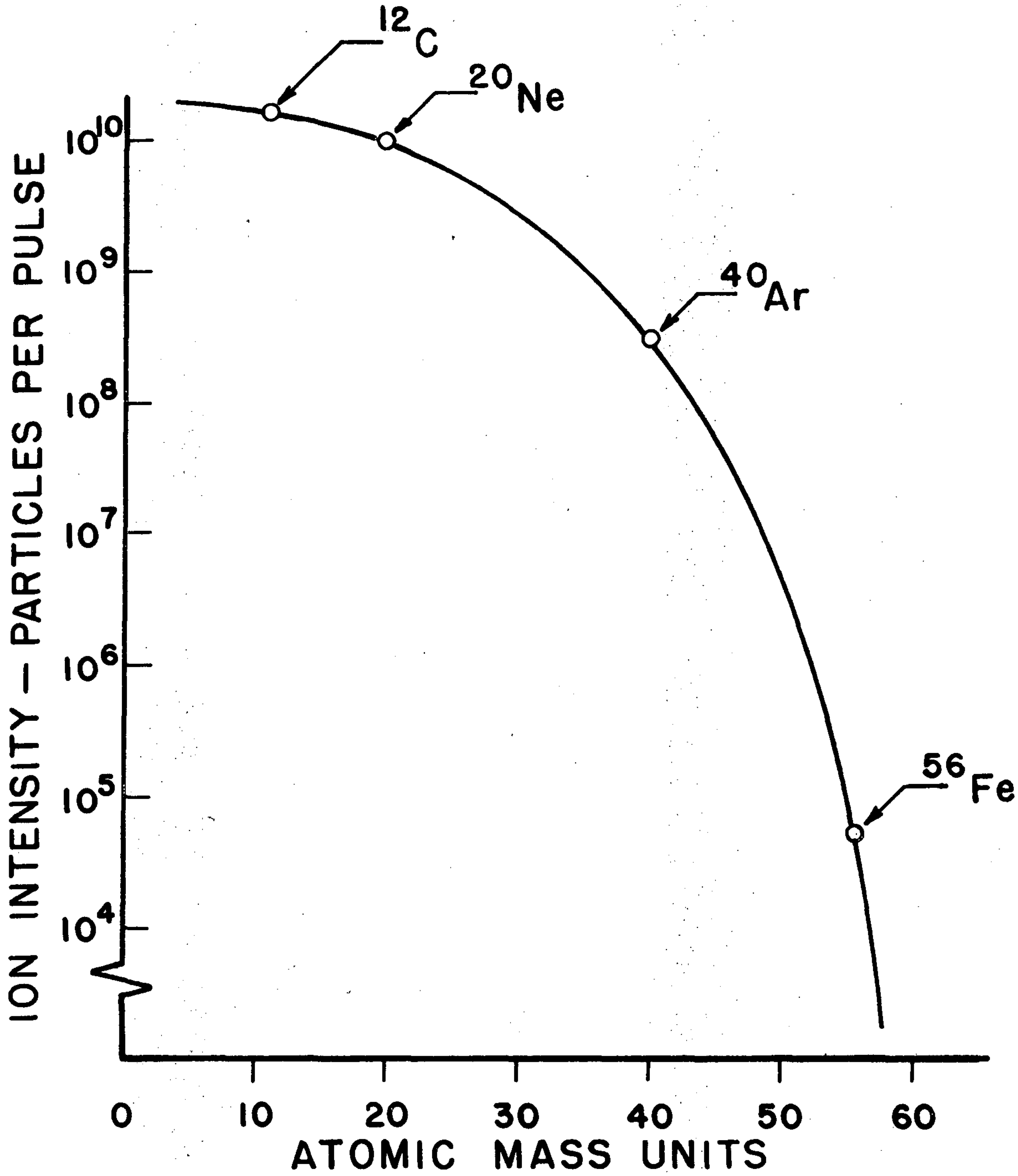

EXPECTED BEVALAC ION INTENSITIES
(FULLY STRIPPED IONS)

XBL 732-209

Fig. 2

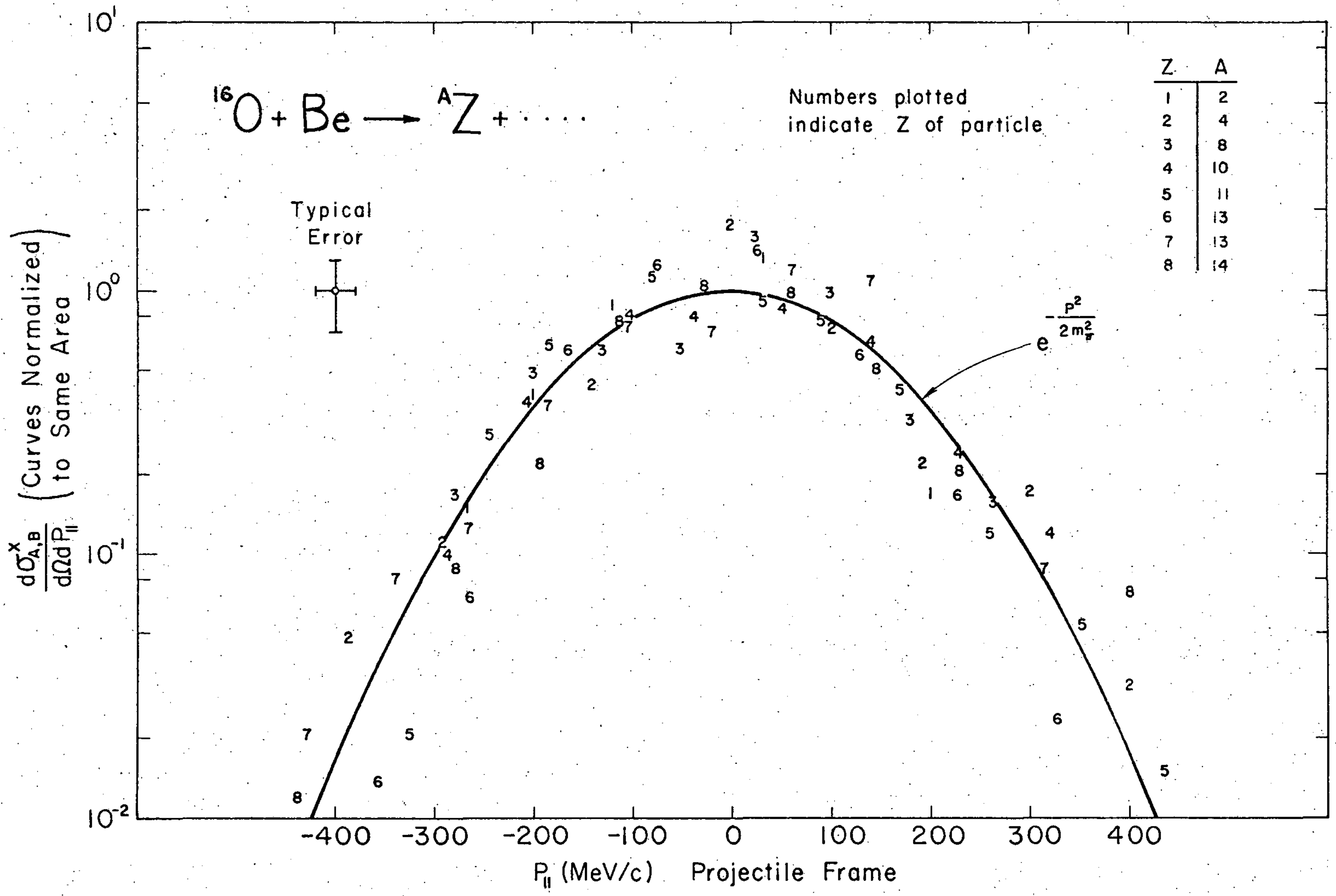

XBL 736-779

Fig. 3

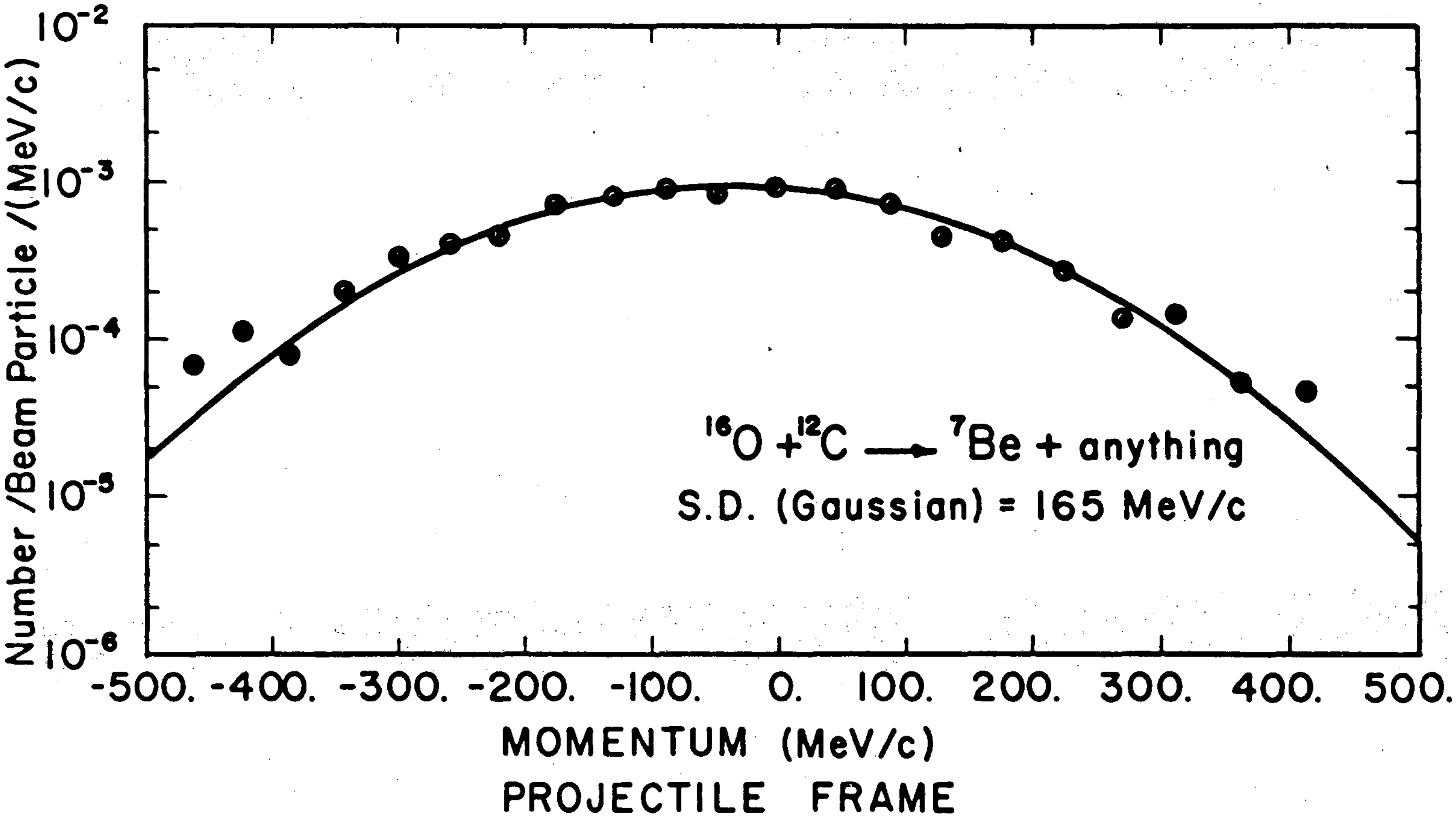

XBL 7411-8579

Fig. 4

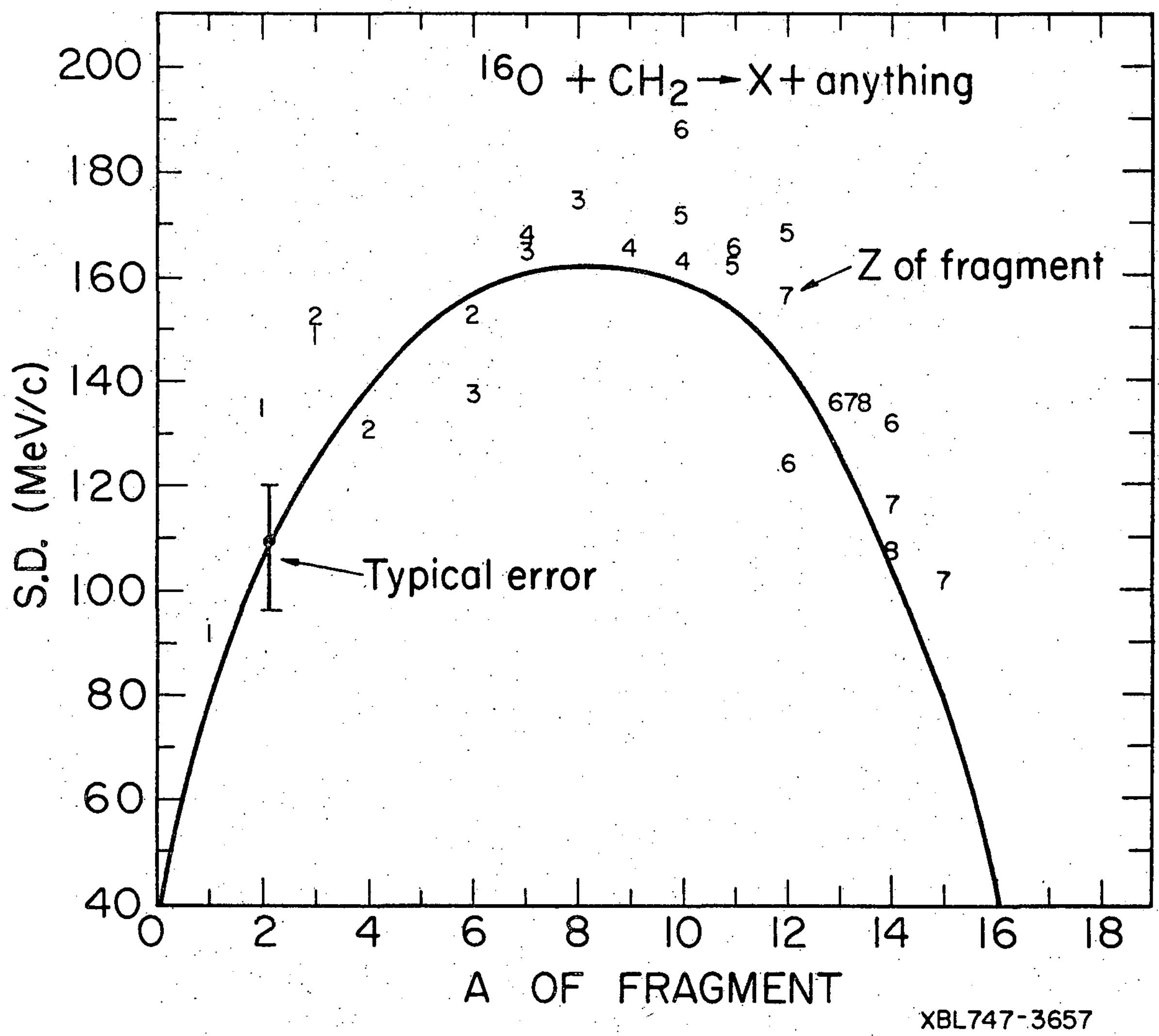

$^{16}O + CH_2 \rightarrow X +$ anything
Z of fragment
Typical error
S.D. (MeV/c)
A OF FRAGMENT
XBL747-3657

Fig. 5

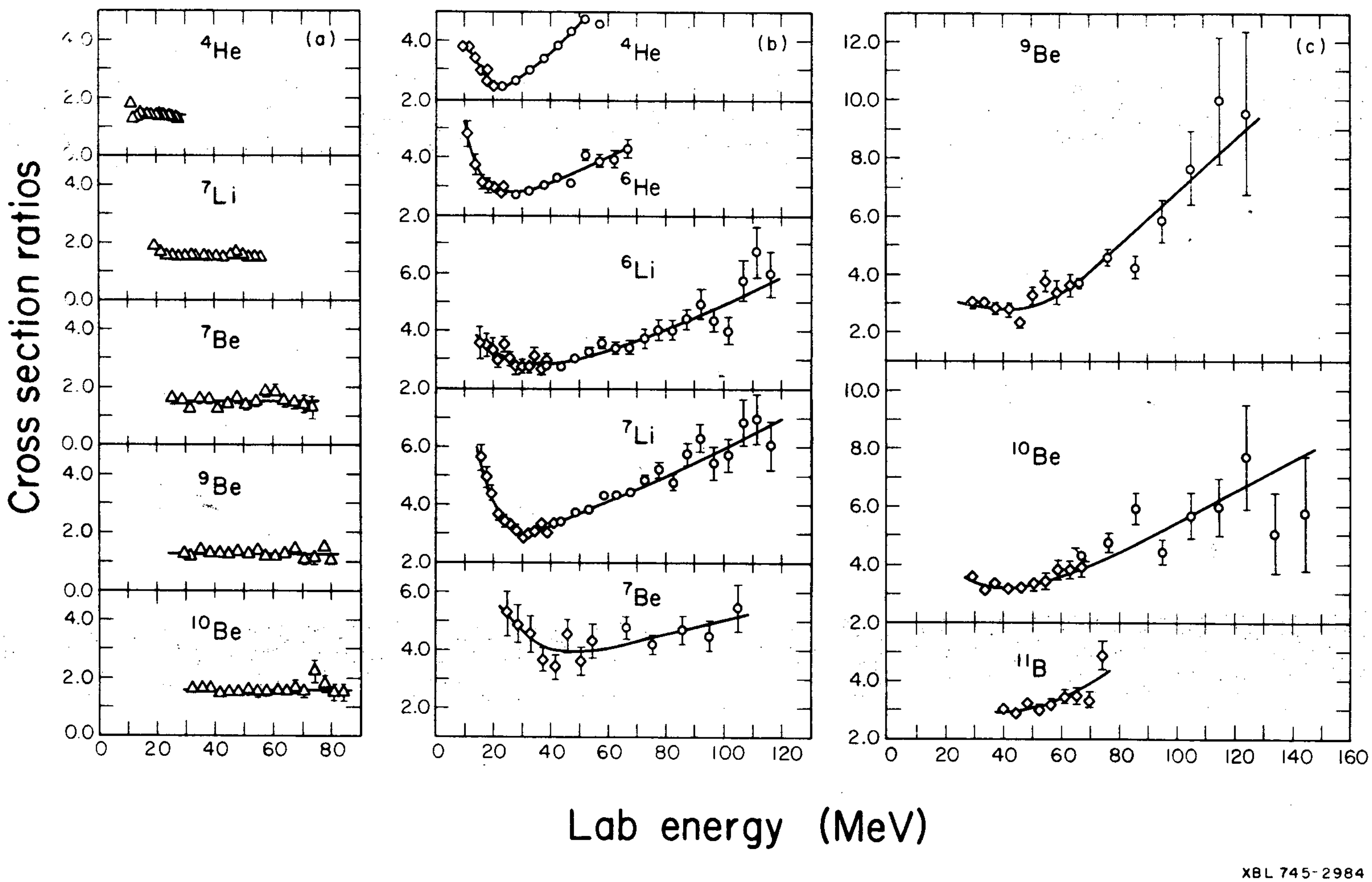

Cross section ratios
Lab energy (MeV)
(a)
(b)
(c)
4He
7Li
7Be
9Be
10Be
6He
6Li
11B
XBL 745-2984

Fig. 6

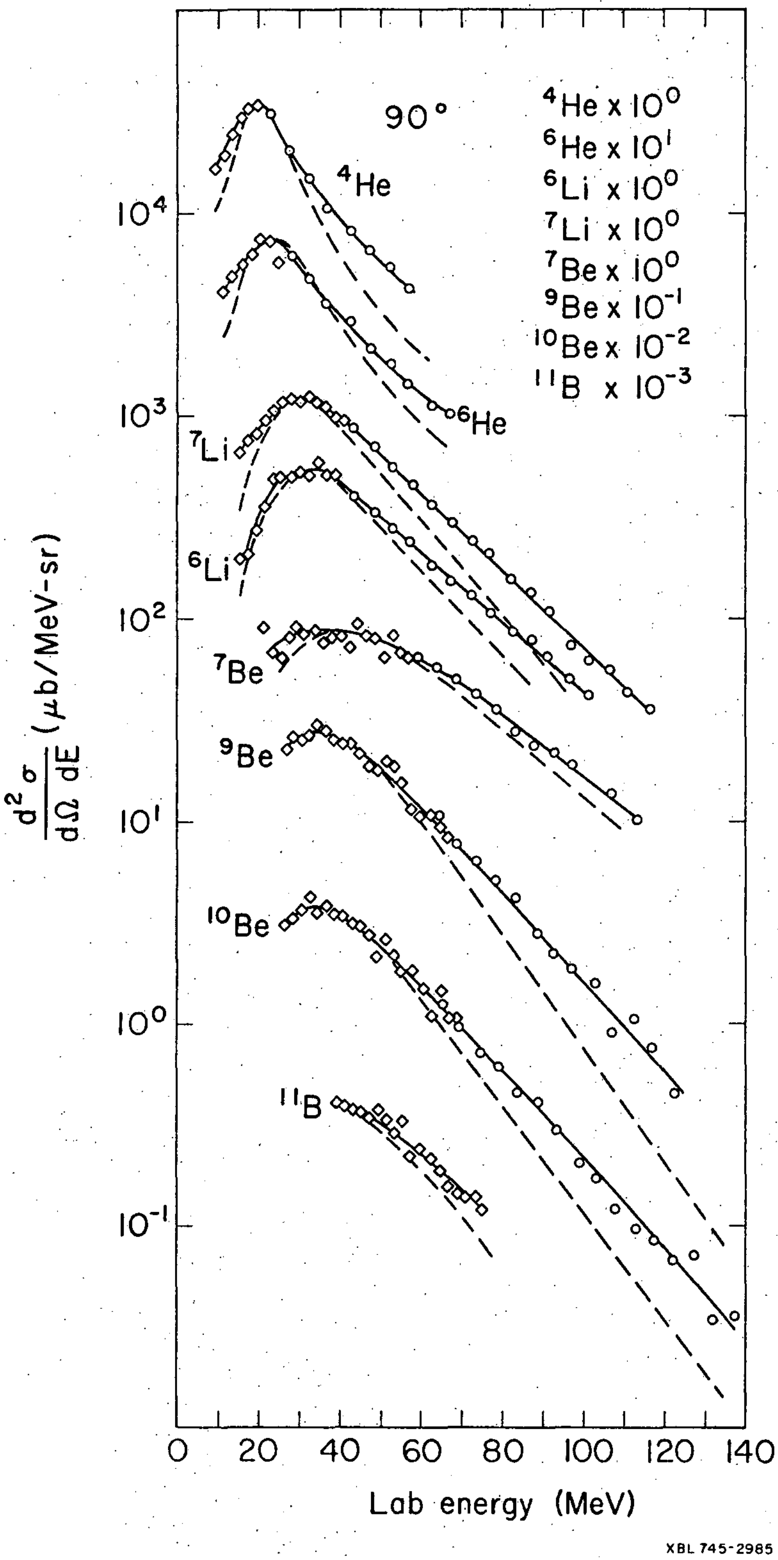
90°
^{4}He x 10^0
^{6}He x 10^1
^{6}Li x 10^0
^{7}Li x 10^0
^{7}Be x 10^0
^{9}Be x 10^{-1}
^{10}Be x 10^{-2}
^{11}B x 10^{-3}
^{4}He
^{6}He
^{7}Li
^{6}Li
^{7}Be
^{9}Be
^{10}Be
^{11}B
$\frac{d^2\sigma}{d\Omega\, dE}$ (μb/MeV-sr)
10^4
10^3
10^2
10^1
10^0
10^{-1}
0 20 40 60 80 100 120 140
Lab energy (MeV)
XBL 745-2985

Fig. 7

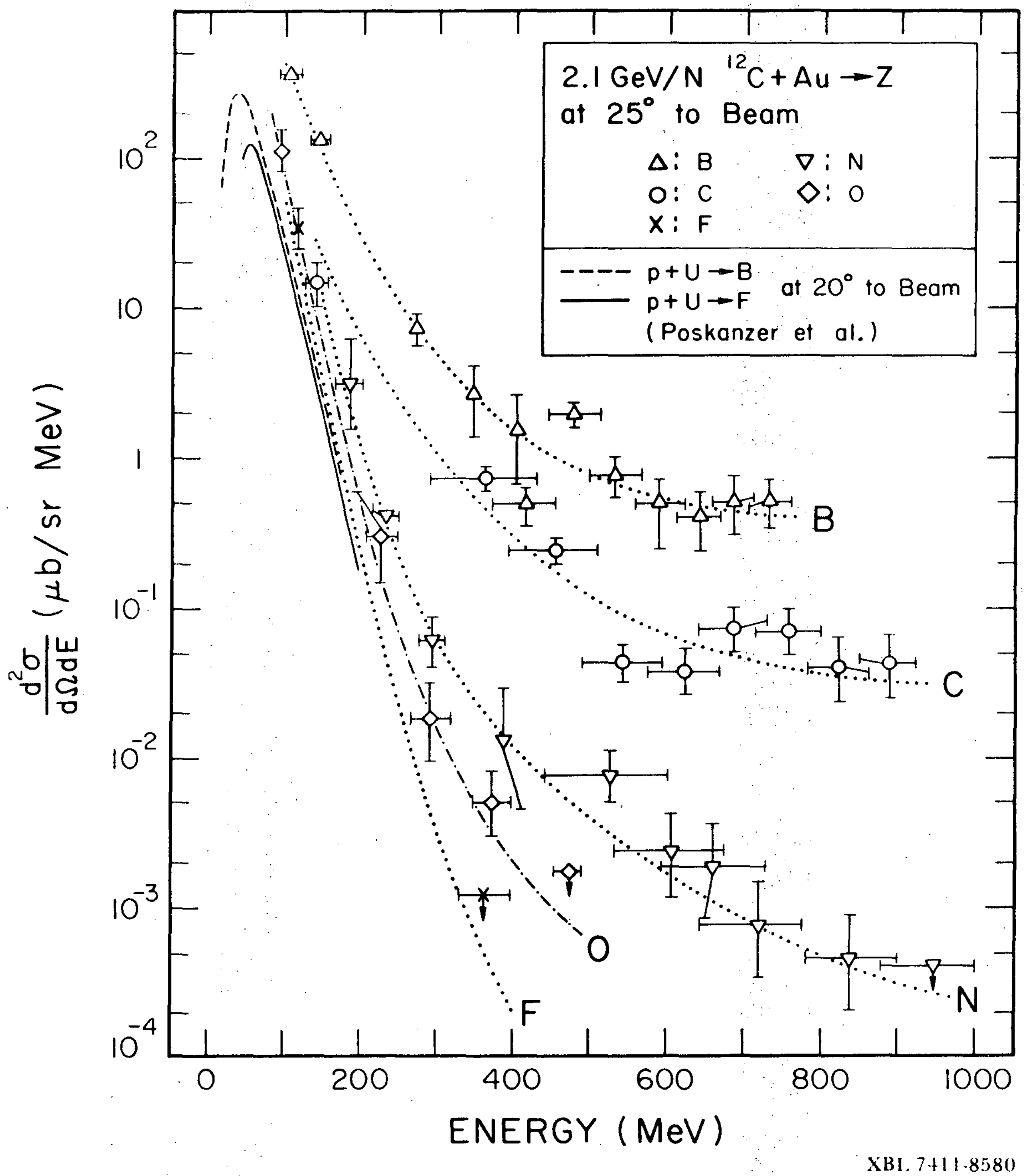

2.1 GeV/N ^{12}C + Au → Z
at 25° to Beam
Δ: B
▽: N
O: C
◇: O
X: F
p + U → B
p + U → F
at 20° to Beam
(Poskanzer et al.)
B
C
N
O
F
10^2
10
1
10^{-1}
10^{-2}
10^{-3}
10^{-4}
$\frac{d^2\sigma}{d\Omega dE}$ (μb/sr MeV)
0
200
400
600
800
1000
ENERGY (MeV)
XBL 7411-8580

Fig. 8

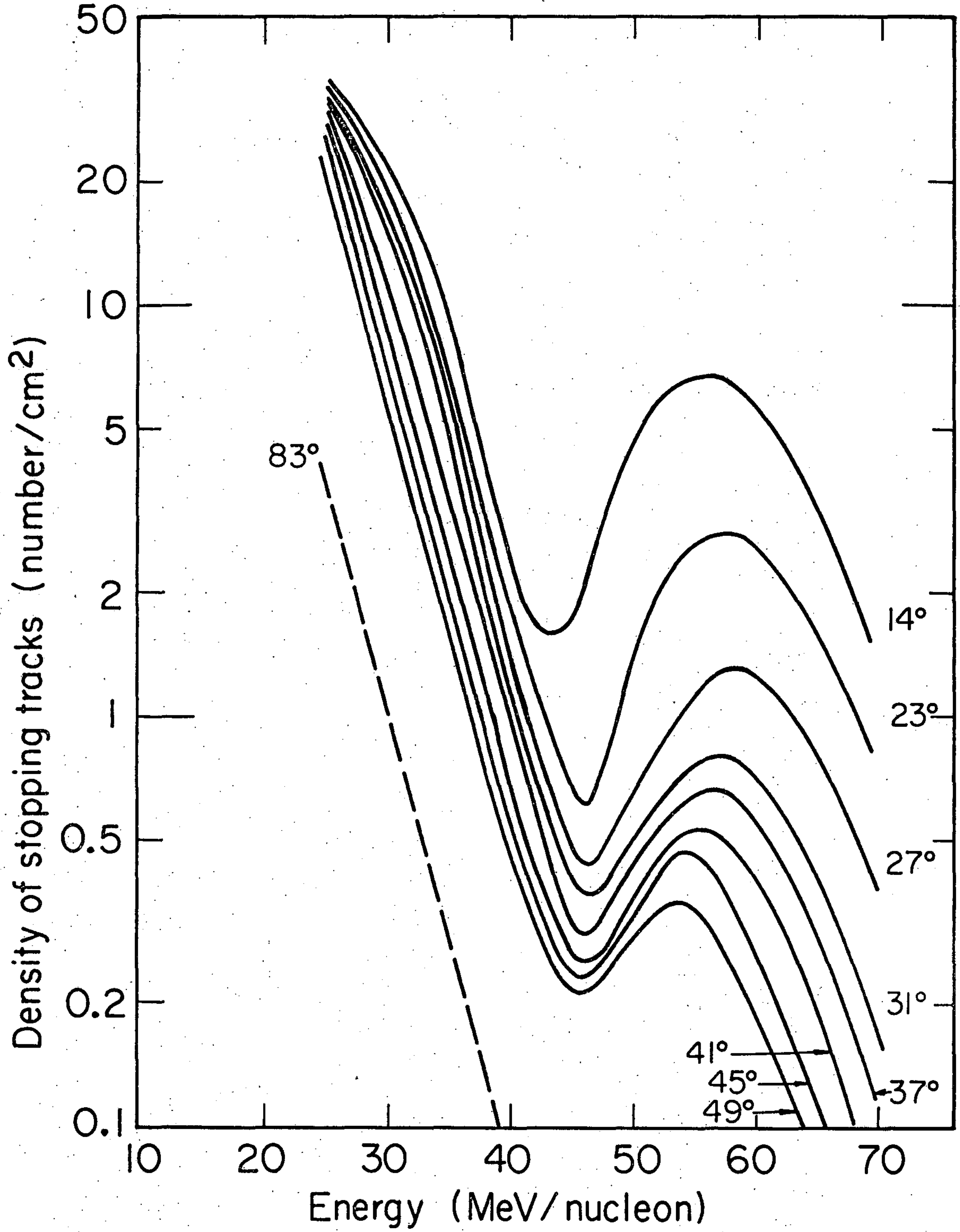

XBL7411-8248

Fig. 9

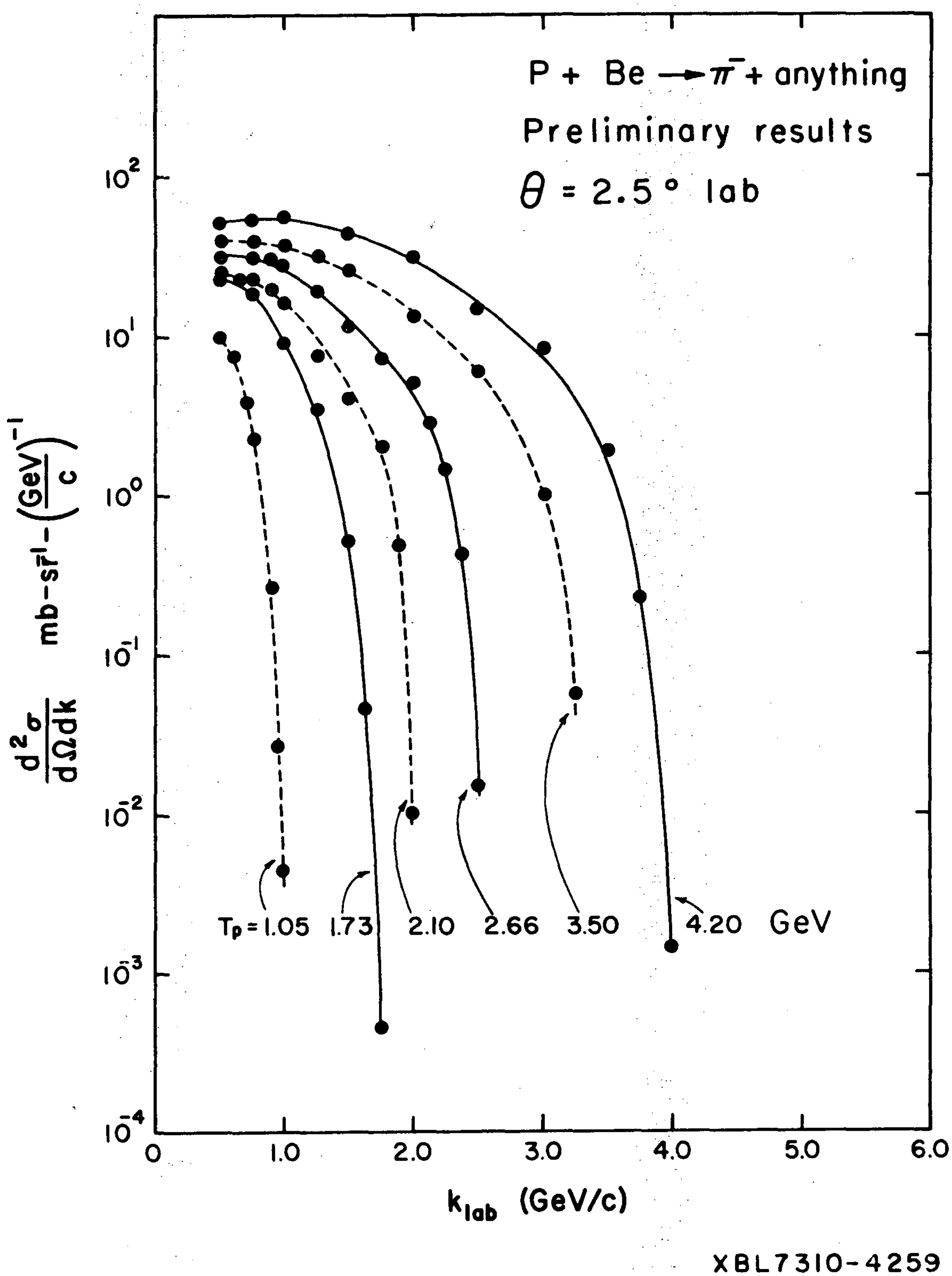
P + Be → π⁻ + anything
Preliminary results
θ = 2.5° lab
d²σ/dΩdk mb-sr⁻¹-(GeV/c)⁻¹
k_lab (GeV/c)
Tp = 1.05
1.73
2.10
2.66
3.50
4.20 GeV
XBL7310-4259

Fig. 10

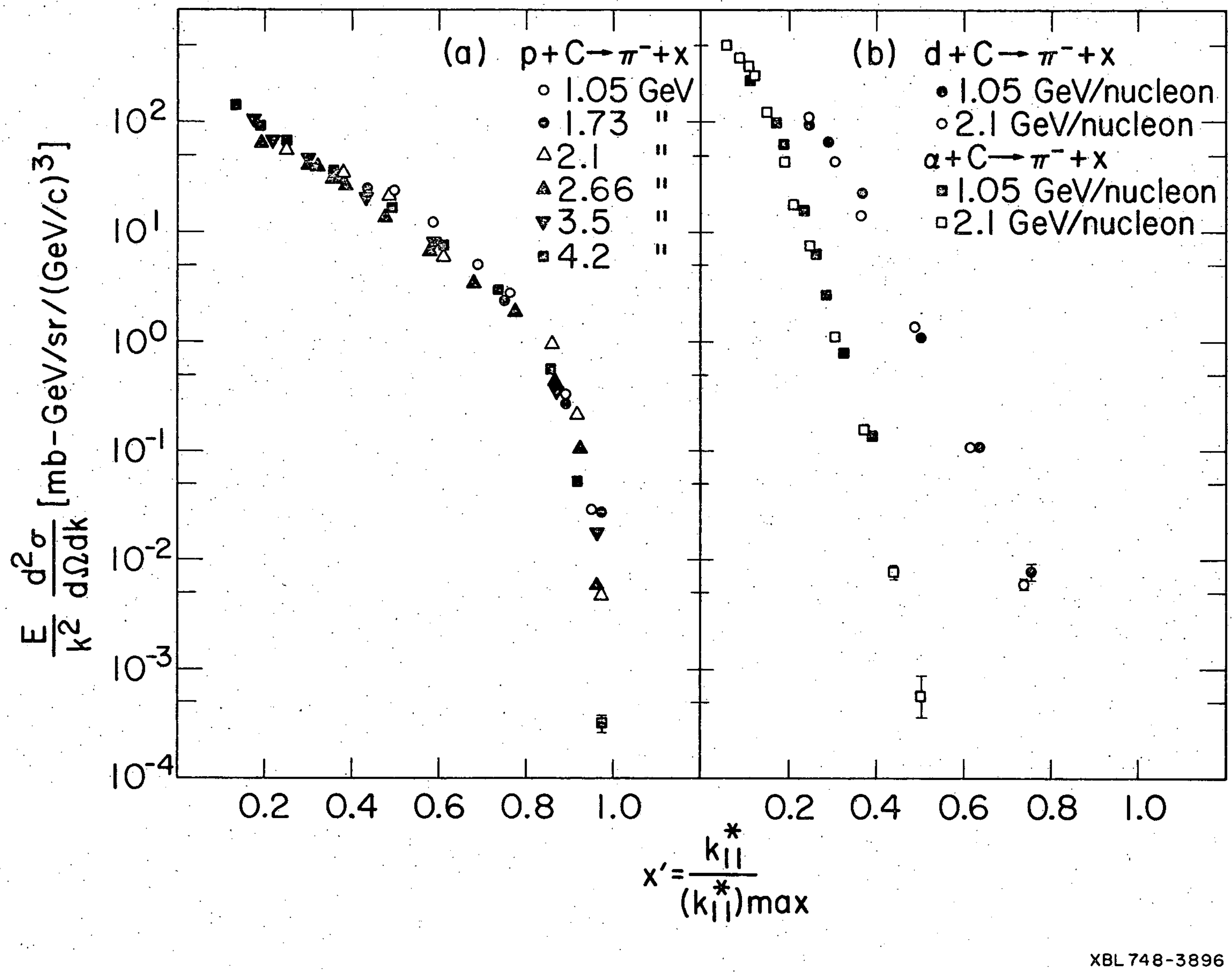
(a) p+C→π⁻+x
○ 1.05 GeV
1.73 "
△ 2.1 "
▲ 2.66 "
▼ 3.5 "
4.2 "
(b) d+C→π⁻+x
● 1.05 GeV/nucleon
○ 2.1 GeV/nucleon
α+C→π⁻+x
1.05 GeV/nucleon
□ 2.1 GeV/nucleon
E/k² d²σ/dΩdk [mb-GeV/sr/(GeV/c)³]
10² 10¹ 10⁰ 10⁻¹ 10⁻² 10⁻³ 10⁻⁴
0.2 0.4 0.6 0.8 1.0
x′ = k*∥/(k*∥)max
XBL 748-3896

Fig. 11

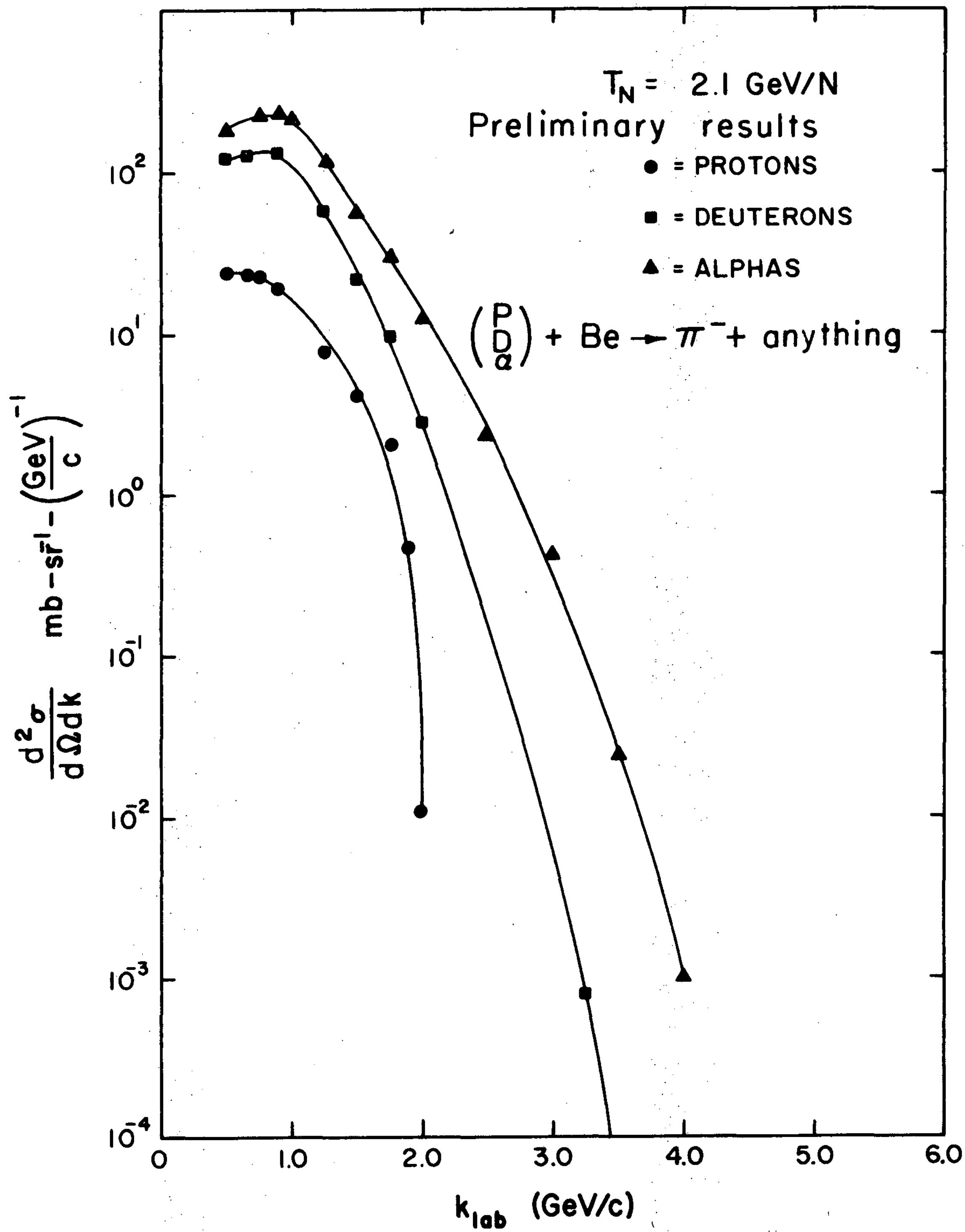

XBL7310-4261

Fig. 12

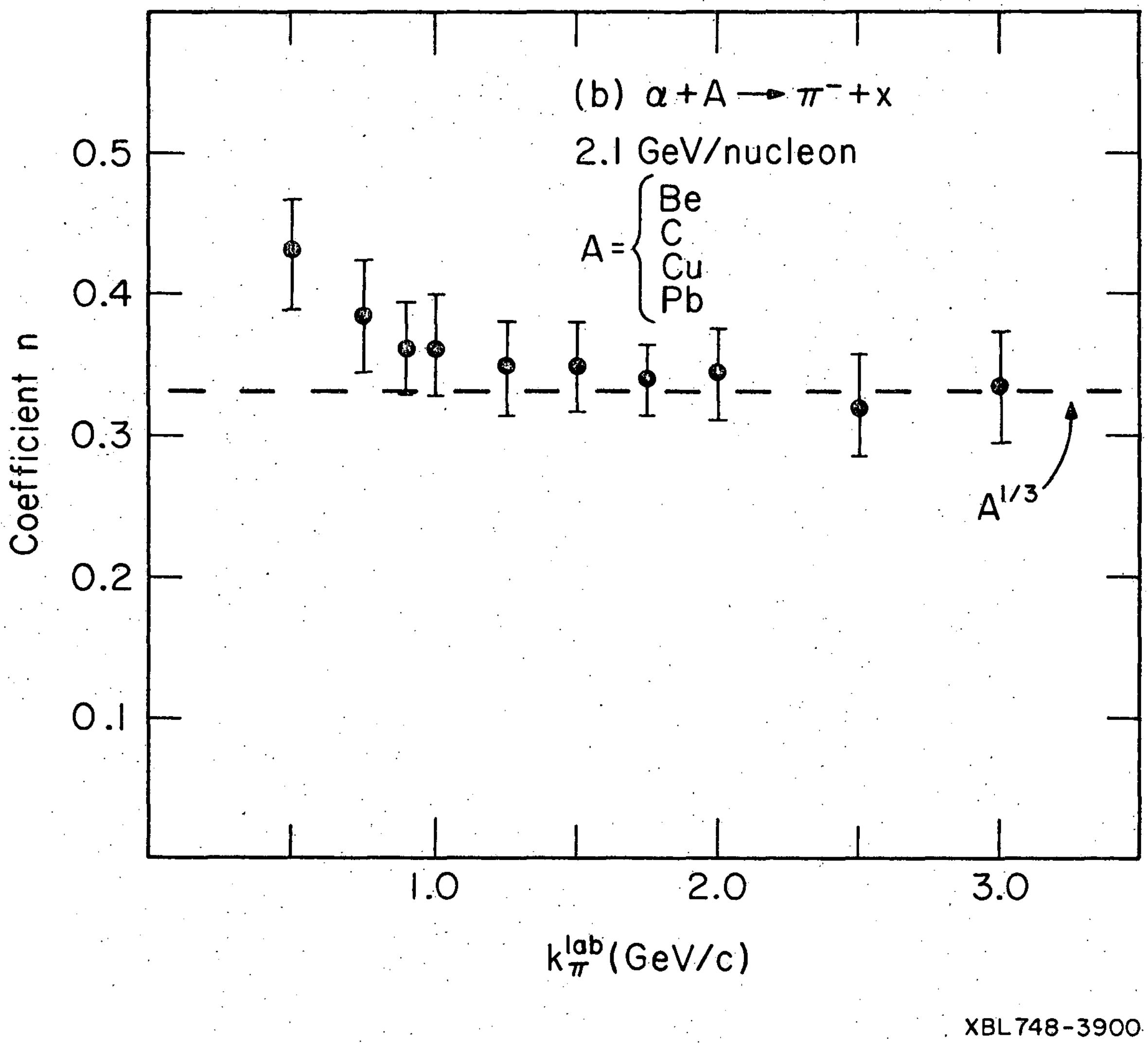
(b) α+A → π⁻+x
2.1 GeV/nucleon
A = Be, C, Cu, Pb
A^{1/3}
Coefficient n
0.5
0.4
0.3
0.2
0.1
1.0
2.0
3.0
k_π^lab (GeV/c)
XBL748-3900

Fig. 13

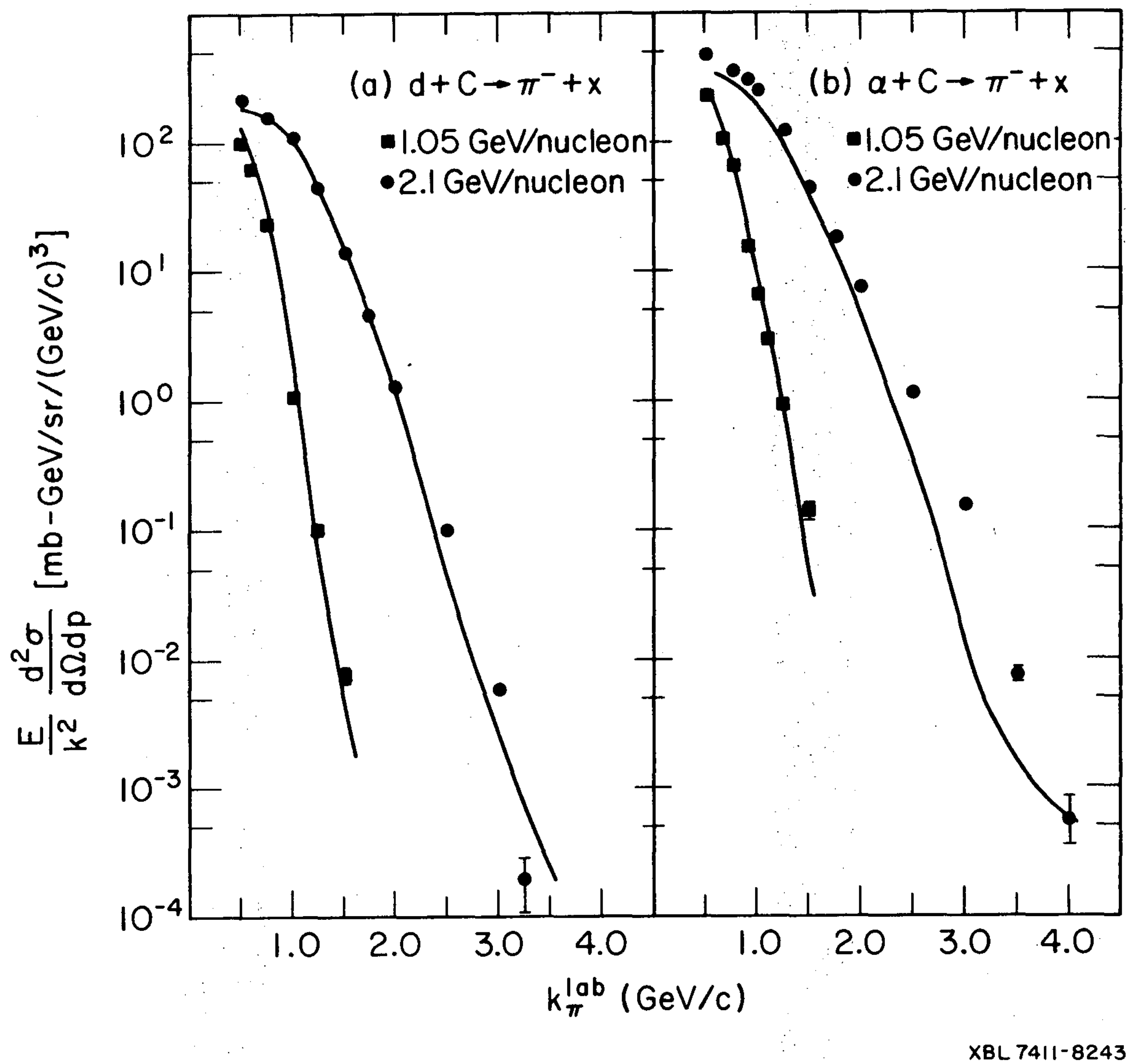

(a) d+C → π⁻ + x
■ 1.05 GeV/nucleon
● 2.1 GeV/nucleon
(b) α+C → π⁻ + x
■ 1.05 GeV/nucleon
● 2.1 GeV/nucleon
E/k² d²σ/dΩdp [mb-GeV/sr/(GeV/c)³]
10²
10¹
10⁰
10⁻¹
10⁻²
10⁻³
10⁻⁴
1.0
2.0
3.0
4.0
k_π^lab (GeV/c)
XBL 7411-8243

Fig. 14

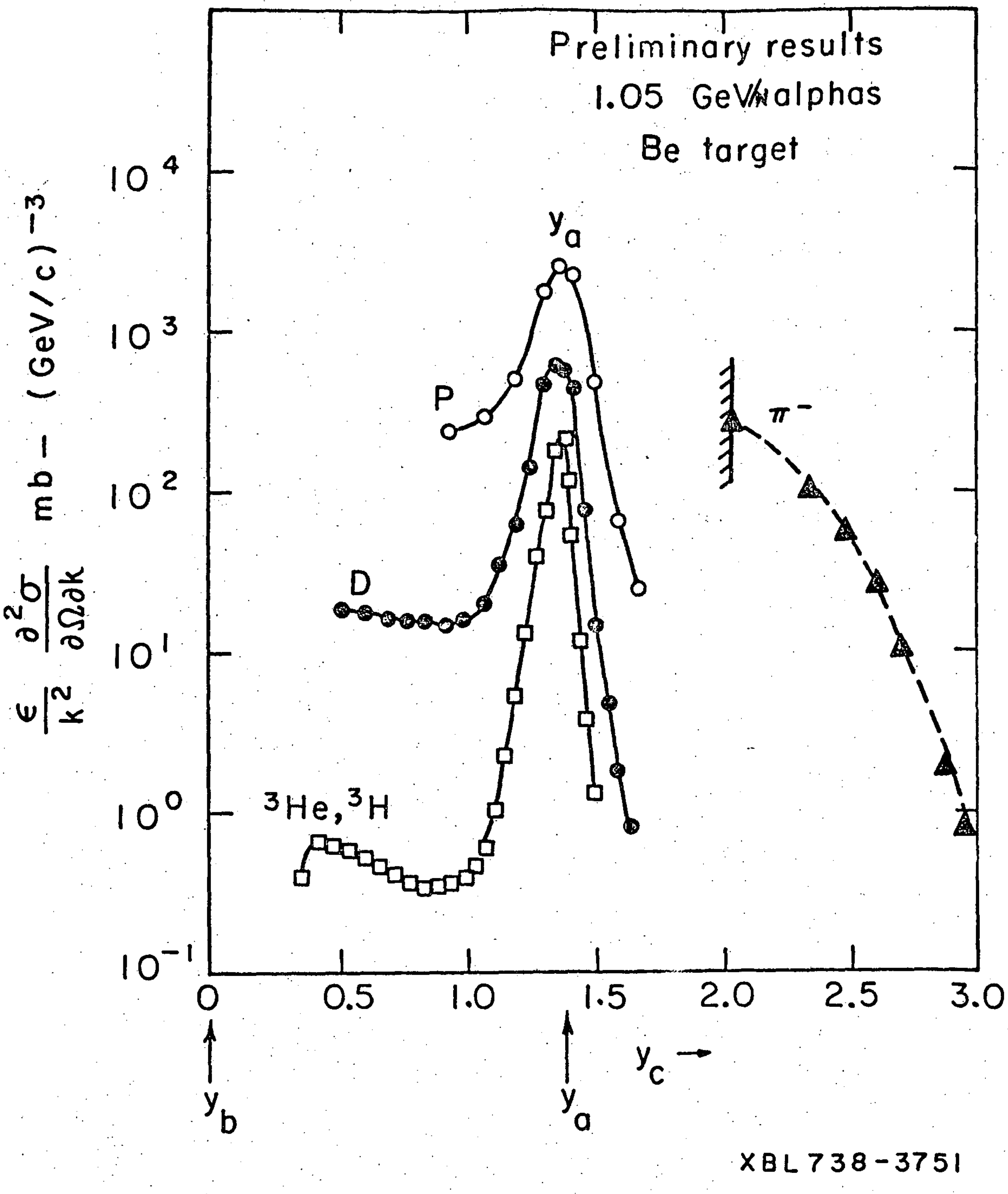

Preliminary results
1.05 GeV/N alphas
Be target
10^4
10^3
10^2
10^1
10^0
10^{-1}
$\frac{\epsilon}{k^2} \frac{\partial^2 \sigma}{\partial \Omega \partial k}$ mb - (GeV/c)$^{-3}$
y_a
P
D
^{3}He, ^{3}H
π^-
0
0.5
1.0
1.5
2.0
2.5
3.0
y_b
y_a
y_c
XBL 738-3751

Fig. 15

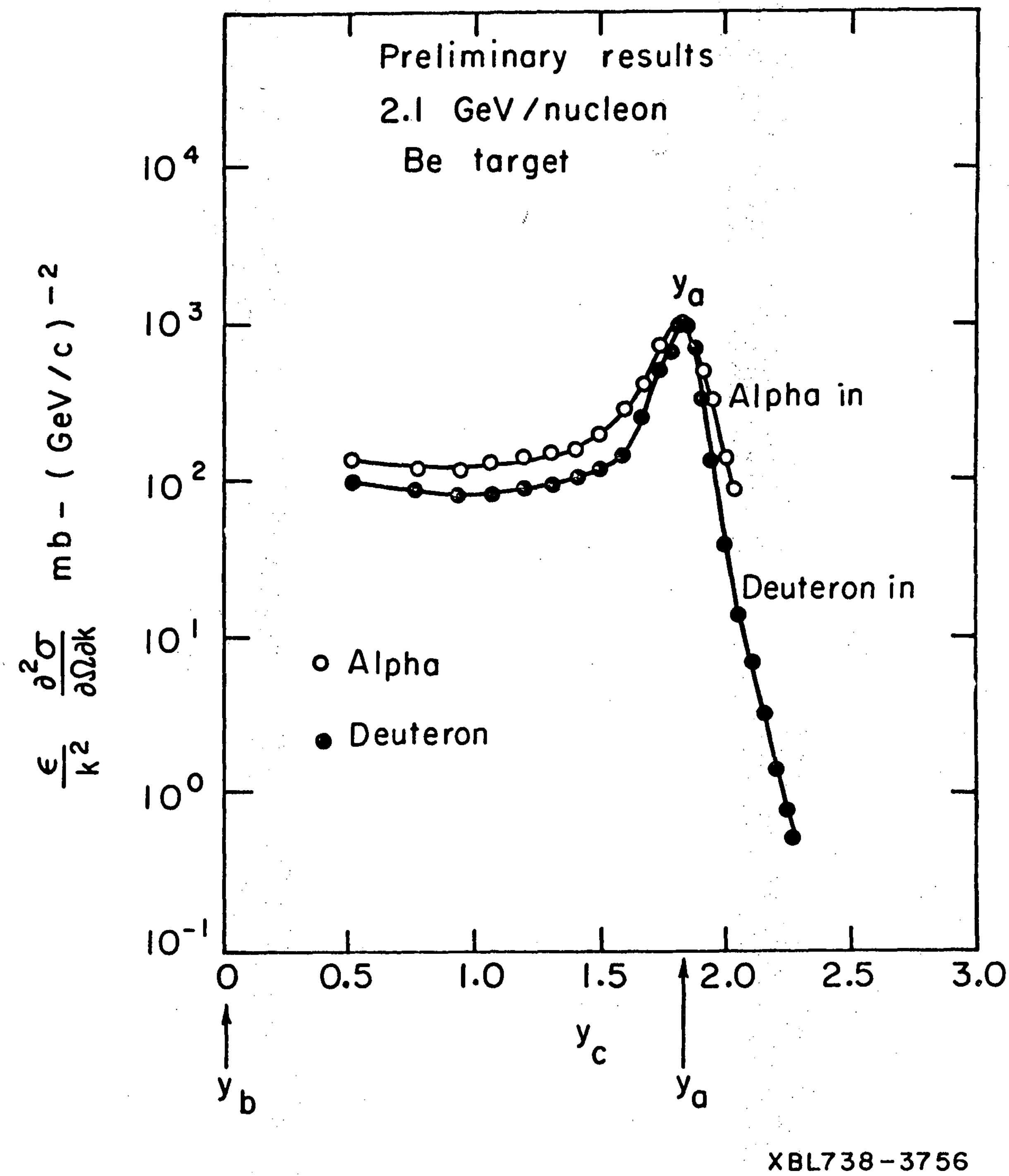
Preliminary results
2.1 GeV/nucleon
Be target
y_a
Alpha in
Deuteron in
Alpha
Deuteron
10^4
10^3
10^2
10^1
10^0
10^{-1}
$\frac{\epsilon}{k^2} \frac{\partial^2\sigma}{\partial\Omega\partial k}$ mb - (GeV/c)$^{-2}$
0
0.5
1.0
1.5
2.0
2.5
3.0
y_c
y_b
y_a
XBL738-3756

Fig. 16

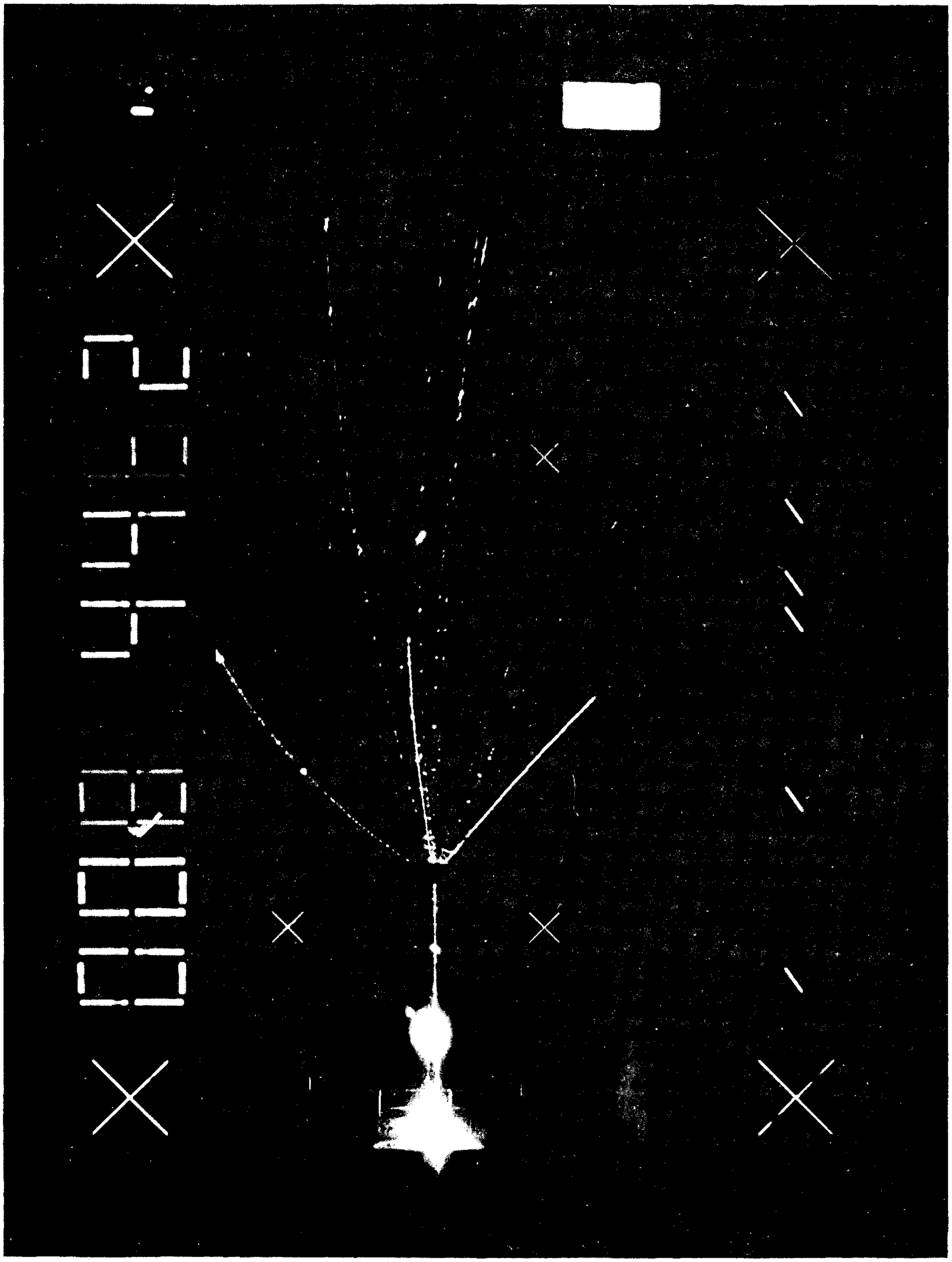

XBB 748-5728

Fig. 17

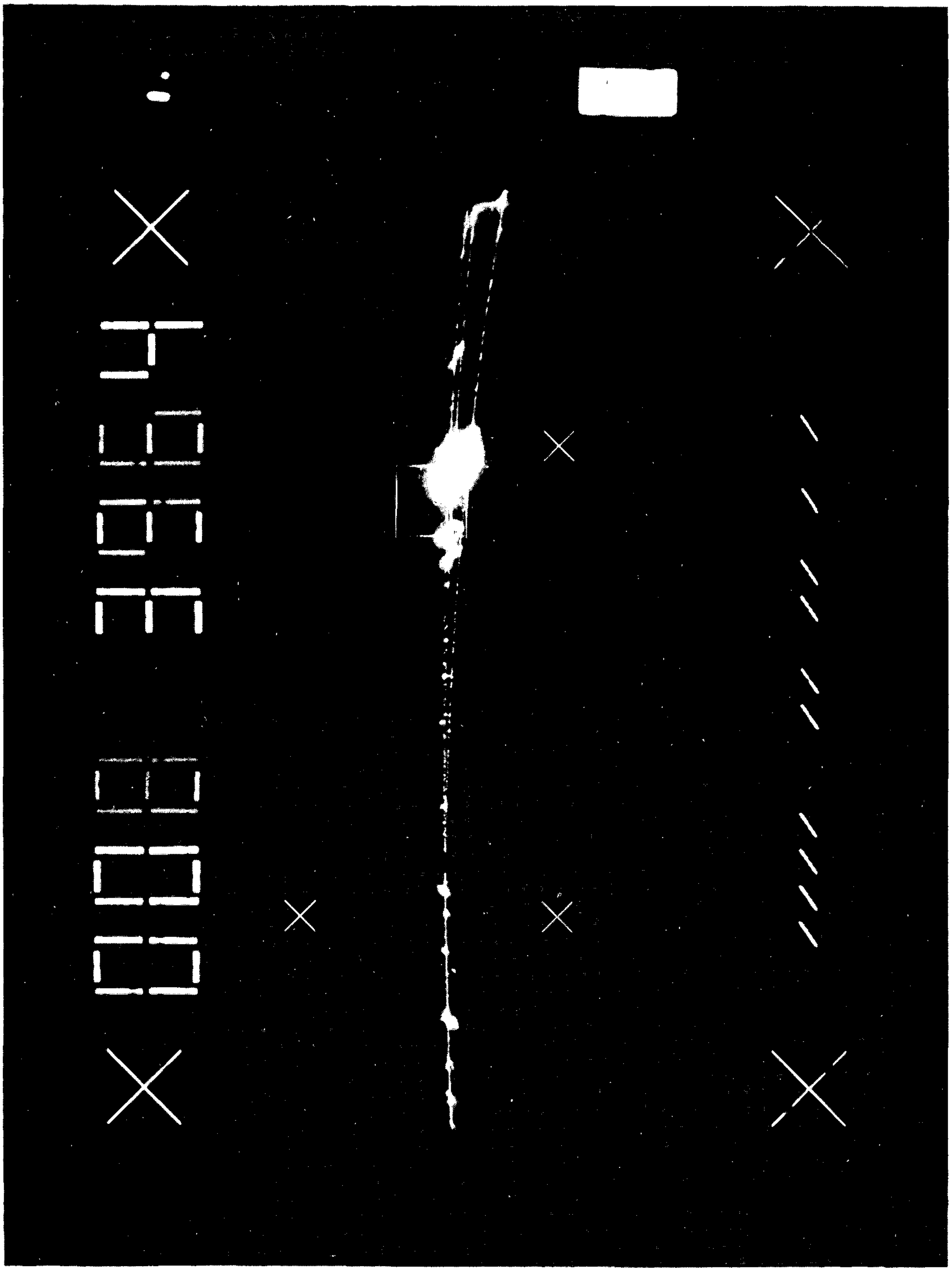

XBB 748-3722

Fig. 18

TECHNICAL INFORMATION DIVISION
LAWRENCE BERKELEY LABORATORY
UNIVERSITY OF CALIFORNIA
BERKELEY, CALIFORNIA 94720